MATHEMATICAL BIOSCIENCES
AND ENGINEERING
Volume **7**, Number **2**, April **2010**

doi:10.3934/mbe.2010.7.277

pp. **277–300**

A PRESSURE MODEL OF IMMUNE RESPONSE TO MYCOBACTERIUM TUBERCULOSIS INFECTION IN SEVERAL SPACE DIMENSIONS

Fabrizio Clarelli and Roberto Natalini

Istituto per le Applicazioni del Calcolo "M. Picone", CNR
c/o Dip. di Matematica, Università di Roma "Tor Vergata"
Via della Ricerca Scientifica, 1; I-00133 Roma, Italy

(Communicated by Stephen Gourley)

Abstract. Mycobacterium tuberculosis (Mtb) is a widely diffused infection. However, in general, the human immune system is able to contain it. In this work, we propose a mathematical model which describes the early immune response to the Mtb infection in the lungs, also including the possible evolution of the infection in the formation of a granuloma. The model is based on coupled reaction-diffusion-transport equations with chemotaxis, which take into account the interactions among bacteria, macrophages and chemoattractant. The novelty of this approach is in the modeling of the velocity field, proportional to the gradient of the pressure developed between the cells, which makes possible to deal with a full multidimensional description and efficient numerical simulations. We perform a linear stability analysis of the model and propose a robust implicit-explicit scheme to deal with long time simulations. Both in one and two-dimensions, we find that there are threshold values in the parameters space, between a contained infection and the uncontrolled bacteria growth, and the generation of granuloma-like patterns can be observed numerically.

1. **Introduction.** Tuberculosis (Tb) is a common and deadly infectious disease that is caused by Mycobacterium tuberculosis. The World Health Organization (WHO) has estimated that 1.6 million deaths resulted from Tb in 2005 [25]. Tb is an aerosol-transmitted infectious disease, but, in most cases, it is a curable disease. An important and striking aspect of Tb is that exposure to the bacteria rarely leads to active disease. However, it has been estimated that currently, one third of the world's population is infected with Mtb, but, for most people, innate immunity is effective in clearing the pathogens [7, 8]. Of those individuals unable to clear the bacteria, only a small proportion ($\approx 5\%$) progress to active disease [4]. In the vast majority, adaptive immunity succeeds in containing the pathogen via the formation of lesions called granulomas, resulting in latent infections [5]. Formation and maintenance of a granuloma is thought to play a central role in the ability of the host-immune response to achieve and maintain latency [9]. Approximately 5% to 10% of individuals who initially achieve latency later develop active tuberculosis as a result of reactivation. Reactivation can occur if the immune system is compromised in some way, for example HIV, drugs, aging, or alcohol abuse.

2000 *Mathematics Subject Classification.* Primary: 35K57, 92C17 ; Secondary: 65C20, 93A30.
Key words and phrases. Reaction-diffusion-advection, Mycobacterium tuberculosis, Multidimensional model, Chemotaxis, Internal velocity.

Since the organism is transmitted primarily by the respiratory route, and although it can cause disease in most organs, pulmonary tuberculosis is most common. Initial infection occurs in alveolar region of the lungs. In the case of Mtb, bacteria duplicate themselves in $1-4$ days [11], i.e. they grow very slowly. Doubling times of $24-96$ hours have been reported for Mtb also by [24] [26], and this is striking when one considers that E. coli has a doubling time of as low as 20 minutes. The bacteria growing rate is a key factor that can determine whether the system achieved latent infection or active Tb.

Once infection is present in alveoli, bacteria release a chemokine, see [21], that it is an attractant for macrophages. For this reason, macrophages movements to the site of infection occurs via both random motion (diffusion) and direct cell movement (chemotaxis). Alveolar macrophages interact with bacteria by phagocytosis process [8]. Actually, bacteria replicate also within the macrophage and induce cytokines that initiate the inflammatory response in the lungs. Macrophages and lymphocytes migrate to the site of infection and form a granuloma [5]. The function of the granuloma is to segregate the infection to prevent spread to the remainder of the lung and to other organs, as well as to concentrate the immune response directly at the site of infection. Living bacilli have been isolated from granulomas or tubercles in the lungs of persons with clinically inactive tuberculosis, indicating that the organism can persist in a granulomatous lesion for many years [15, 19]. At the most fundamental level, latent tuberculosis can be viewed as an equilibrium between host and bacillus, where the number of bacteria is stable and low, while, on the other hand, in active Tb state the number of bacteria grows exponentially [11].

Recently, some continuous spatial models were proposed to describe the innate immune response to the infection with Mtb, see for instance [8] and references therein, and were based on reaction diffusion equations, which can be seen as a modified diffusive prey-predator system with chemotaxis. To express the hydrodynamic velocity of the flow, it was used the so-called "no-void" condition, which is the assumption that all the space is filled with both bacteria and macrophages. This condition allows, but only in the one-dimensional case, to compute the velocity by solving a free boundary problem.

However, these models are quite unrealistic. Apart from the quite stringent restriction to a one-dimensional setting, we observe that, in this crowded situation, it is difficult to imagine a Fickian mechanism of diffusion, since the gradient of the density is flat. Moreover, outside of the granuloma, there is no mechanism to describe the generation of macrophages, The external immune respose is just given by the macrophages flow on the free boundary. Now, it is difficult to assess such a flow in practice, and essentially it is left as an arbitrary data of the problem.

To circumvent these difficulties, in this paper we prefer to turn to a more complete hydrodynamical approach by defining the velocity field by a state law. Here we decided to use the Darcy law, as proposed in [1, 6] for the similar framework of tumor growth. This way, we can develop our model in several space dimensions, which was not achievable by using no-void assumption, and it is of great importance for a more realistic fitting of the model. In this new setting, the Fickian movements of cells are perfectly admissible, since the cells just use a fraction of the total volume available. Moreover, reasonable boundary conditions can be assigned, for instance no flux conditions for a closed region or basal concentrations of macrophages for partial subregions of the lung. Anyway, the considered domain is by no means limited to the granuloma, and so it is possible to extend our model to take into

account more general situations as a change in the immunitary response or other external factors.

The paper is organized as follows: in section 2 we outline the dynamics of bacteria, macrophages and chemoattractant. Since the velocity field, in the transport term, is given by a gradient of pressure, we indicate this model as a pressure model. Then, we write the system in a dimensionless form (section 3). In section 4, we discuss the linear stability of the system in one-dimension, by considering homogeneous steady-state solutions and their stability under small non-homogeneous perturbations. In section 5, we describe a numerical schemes to simulate the model. We developed explicit and implicit-explicit (IMEX) numerical schemes, the second one are useful to have a better numerical stability, necessary to obtain simulations for a long time period (months or years), see [20]. Hence, we investigate numerically the stable and unstable regions in the nonlinear case. Finally, in section 6, we extend the model in 2-dimensions. Here, we propose simulations of the model under different conditions. In the long time simulations, we consider also the strengthening (adaptive immune response) and the weakening of the immune system (drug or alcohol abuse, immune system diseases etc.) choosing a variable killing rate of bacteria and a variable death rate of macrophages. Then, we identify a range of parameters, which correspond to a persistent pattern formation in the solutions. This pattern is given by an equilibrium state between bacteria and macrophages, which is equivalent in the mathematical model to the formation of granuloma.

2. **The mathematical model.**

In this section, we introduce and develop a mathematical model able to describe, in a simple way, the innate response of human immunity system to Mtb infection. To describe this process, we assume that a droplet of Mtb is inhaled. Once bacteria are in the lungs, they begin to duplicate and produce chemoattractant, so that macrophages, randomly distributed, are attracted toward bacteria by chemotaxis movement. When macrophages meet bacteria, they can kill bacteria with more or less effectiveness.

The simplicity of our approach, is due to the fact that we deal with bacterium-macrophage interaction as a sort of prey-predator modified system. For this reason, we use reaction-advection-diffusion equations with coupled chemotaxis terms, describing as these unknowns interact, move, die and proliferate. These equations are obtained by a mass balance of bacteria, macrophages and chemoattractant. The transport term is due to the the pressure of macrophages and bacteria, which "push each other". This assumption seems to be more realistic, and yields a model in several space dimensions.

In order to describe the governing equations of the system, the concentration of chemoattractant $[g/cm^3]$ is indicated by C, the number of bacteria and macrophages per volume $[\#/cm^3]$ is indicated by B and M respectively (knowing that the mass density of a single bacterium ρ_B and macrophage ρ_M can be considered constant).

2.1. **Bacteria.**

Bacteria can move via diffusion and passive transport, they reproduce and can be killed by macrophages. We consider, with $B(x,t)$, an average behavior of all bacteria, using as reproducing parameter (α) an average rate. By a mass balance of bacteria, we obtain the following equation

$$B_t + \overbrace{\nabla\cdot(v_B B)}^{\substack{Advection\\ term}} = \overbrace{D_B\Delta B}^{\substack{Bacterium\\ diffusion}} + \overbrace{\alpha B}^{\substack{Bacterium\\ reproduction}} - \overbrace{\lambda BM}^{\substack{Bacterium\\ clearing}}, \tag{1}$$

where $\nabla \cdot (v_B B)$ is the advection term due to the average velocity v_B, which is to be determined. $D_B \Delta B$ represents the random diffusion of bacteria, see also [8], α is the replication rate and λ is the death rate due to the interaction with macrophages. The last one, λ, is a sort of efficiency indicator of immune system, for this reason we choose its value in each simulation.

2.2. **Macrophages.** Here, we consider only the innate immunity response, i.e. we do not include activated macrophages, which require T cells for activation. Macrophages can move via diffusion, transport and chemotaxis, and they die with a rate μ. Making a mass balance, the equation governing the dynamics of the macrophage population is given by

$$M_t + \overbrace{\nabla \cdot (v_M M)}^{\substack{Advection \\ term}} = \overbrace{D_M \Delta M}^{\substack{Macrophage \\ diffusion}} - \overbrace{\chi \nabla \cdot (M \nabla C)}^{chemotaxis} - \overbrace{\mu M}^{\substack{Macrophage \\ death}} \quad ; \tag{2}$$

where $\nabla \cdot (v_M M)$ is the advection term due to the average velocity v_M to be determined, $D_M \Delta M$ represents the random diffusion of macrophages, $\chi \nabla \cdot (M \nabla C)$ is the chemotactic term, for a detailed description see [10]. μ is the death rate of macrophages, due to the natural decay and to the interactions with bacteria.

2.3. **Chemoattractant.** The chemoattractant $C(x,t)$ is produced by extracellular bacteria B, at a maximal rate σ_B. It comes from a Michaelis-Menten type equation, where σ_B represents the saturation. Moreover, chemoattractant diffuses at a rate D_C. It has a natural decay rate, $\Gamma_C C$, and is used by macrophages M, at a rate Γ_M. The governing equation for chemoattractant $C(x,t)$ is

$$C_t = \overbrace{D_C \Delta C}^{\substack{Chemoattractant \\ diffusion}} + \overbrace{\sigma_B \frac{B}{B + b_0}}^{\substack{Chemoattractant \\ production}} - \overbrace{\Gamma_C C}^{\substack{Natural \\ decay}} - \overbrace{\Gamma_M M C}^{\substack{Macrophage \\ uptake}} . \tag{3}$$

2.4. **Initial and boundary conditions.** In lungs there is a background level of macrophages, which are present in alveolar tissue and patrol for foreign particles. The total number of alveolar macrophages in the human lung, see [9], is estimated to be between 10 and 100 alveolar macrophages per mm^2 of alveolar tissue.

Furthermore, we can guess that the initial infection of bacteria can be given by even 10 bacteria or more. On the boundary of the region considered, we assume to have no-matter exchange, as first approach. It means that the normal flux is zero, indicating by $\mathbf{n}$ the normal vector, the **boundary conditions** are

$$\mathbf{n} \cdot \nabla C = \mathbf{n} \cdot \nabla M = \mathbf{n} \cdot \nabla B = 0, \ at \ \partial\Omega. \tag{4}$$

For the initial conditions we take

$$C(0,x,y) = C_0(x,y), \ B(0,x,y) = B_0(x,y), \ M(0,x,y) = M_0(x,y). \tag{5}$$

2.5. **A pressure equation for the velocity field.** To close the system (1, 2, 3), we have to define the velocity fields v_B and v_M. Several constitutive equations can be formulated, but unfortunately it is not easy to find reliable experimental data on the mechanical characteristics of cells. In absence of experimental evidence, in the following we adopt the simplest constitutive equation possible: i.e. the transport velocity is proportional to the gradient of pressure exercised by the cells among them. This kind of description comes from a momentum balance and a complete description of this approach can be found in [1] [2], [18], and [6]. In this paper we adopt the description previously proposed in [1], where a cell-to-cell interaction

occurs in a tumor spheroid. We adapt this concept to our problem, in which bacteria interact with macrophages.

First, let us consider a single type of cell, characterized by the volume fraction of cells F. The action of the surrounding cells will be described by the scalar quantity $P(F)$, depending only on their local density. $P(F)$ represents the pressure value given by the number of particles by unitary volume, i.e., in a fixed volume. The function P will be monotone increasing in F; i.e.: if we have a greater number of particles, the corresponding pressure will be greater. When we multiply each particle by its single volume, we get the fraction of volume filled by one type of particle, and the corresponding pressure is proportional to the fraction volume. For increasing volume ratio, cells are compressed and the gradient of pressure is greater than zero, so that a repulsive force is increasing and cells tend to move toward a region with a smaller density. Following [6], [1], we model this behavior using Darcy's law, i.e.: assuming that the velocity field is given by:

$$v = -K\nabla P(F), \tag{6}$$

where K is the motility coefficient depending on the medium in which particles move, and we assumed $v_M = v_B = v$. Now, we have to choose a functional form for $P(F)$. We know that the pressure increases with the fraction of volume F of particles interacting, thus we can assume that the F has a maximum at $F_{max} = 1$ (the fraction of volume has to be ≤ 1). Set $F = F_B + F_M$, we have neglected the volume contribution of chemoattractant C. For the sake of simplicity, we choose a linear form for the pressure equation, so that we get

$$P(F) = k_1 F. \tag{7}$$

Notice that it should be possible to refine our approach, by introducing a threshold value of volume fraction called $\bar{F}$; below this threshold value we set $P(F) = 0$, above this value we have $P(F) > 0$. Namely, the threshold value is the undeformed state, and corresponds to the density of cells, such that no action is exerted on their neighbors. Here we have just set the threshold value $\bar{F} = 0$, but the general case could be considered by the same ideas as in the following.

Now, $F_B = \hat{B}$ and $F_M = \hat{M}$, where $\hat{B}$ and $\hat{M}$ are bacteria and macrophages fractions of volume, as we will see better in the next section. So, we can write the velocity equation

$$v = -K\left(\nabla\hat{B} + \nabla\hat{M}\right). \tag{8}$$

Remark 1. In a more general framework it would be assumed $v_B \neq v_M$, but this would mean to have $v_B = -K_B\left(\nabla\hat{B} + \nabla\hat{M}\right)$ and $v_M = -K_M\left(\nabla\hat{B} + \nabla\hat{M}\right)$. Since the coefficient K depends on the medium in which the particles move (the same) and the particles themselves, we need to know their behavior. The lack of experimental data regarding the differences in the motion of bacteria and macrophages in the same medium, and the approximations of our model induced us to assume the (8).

2.6. **Parameters.** The choice of parameters is a very hard problem to solve. For this reason we followed the values found in the literature, when available, and by rough estimations otherwise.

We know that the volume of alveolar macrophage is $V_M \approx 10^{-15}$ $[m^3]$ (see [8]), i.e., in 1-D, $V_M^{1D} \approx 1 \cdot 10^{-5}$ $[m]$. A bacterium has a length of about $1 \cdot 10^{-6}$ $[m]$, then, in 1-D, $V_B^{1D} \approx 1 \cdot 10^{-6}$ $[m]$.

The first parameter to know is the replication rate of bacteria: α. Mtb duplicate in $1-4$ days [11], [24] and [26]. Then, if the duplication time is $t^* = 20$ hours (i.e. $7,2000 \cdot 10^4$ seconds), or $t^* = 96$ hours (i.e. $3,456 \cdot 10^5$ seconds), we find α_{20} or α_{96} respectively, given by

$$\alpha_{20} = \frac{Log(2)}{72000} = 9.6 \cdot 10^{-6}\ [1/s],\ \alpha_{96} = \frac{Log(2)}{345600} = 2 \cdot 10^{-6}\ [1/s]. \tag{9}$$

The diffusion coefficients regarding bacteria (D_B), macrophages (D_M) and chemoattractant (D_C), are given in [16], [17], [8]. The chemotactic coefficient is difficult to estimate, because it is a problem to find in literature how infection can affects the chemotactic movement of the macrophages. Following the indications of [8], we choose the simplest option of assuming that uninfected macrophages have a constant chemotactic coefficient χ. Some indications are in [13], [16], [17], [22]. Regarding Γ_M, Γ_C, σ_b and b_0 we follow indications of [8]. The macrophage death coefficient μ is considered smaller than the value given in [8], we make this assumption because in our model we assume no-flux of matter from external boundary. To estimate the value of K, the motility coefficient, we follow the discussion in [1] and references therein. Finally, the coefficient describing the efficiency λ of clearing bacteria is considered as a parameter, typical of a given situation, and it is given from time to time in each simulation. Parameters are listed in table 1.

TABLE 1. Parameters (dimensional) table

Param.	value	Indications	Source
V_M	$10^{-5}\ [m]$	Macrophage volume	[12]
V_B	$10^{-6}\ [m]$	Bacterium volume	[8]
L	$0.1\ [m]$	Domain length	hypotheses
D_M	$10^{-11}\ \left[m^2/sec\right]$	Macrophage diffusion	[23]
D_B	$10^{-13} - 10^{-14}\ \left[m^2/sec\right]$	Bacterium diffusion	[8]
D_C	$10^{-9}\ \left[m^2/sec\right]$	Chemoattr. diffusion	[8]
α	$5 \cdot 10^{-6}\ [1/sec]$	Bacteria reprod.	section 2.1
Γ_M	$1 \cdot 10^{-22}\ [Vol/sec]$	Chemoattr. consumpt.	[8]
Γ_C	$1 \cdot 10^{-8}\ [1/sec]$	Chemoattr. decay	[8]
σ_b	$1 \cdot 10^{-16}\ \left[Vol^{-1}sec^{-1}\right]$	Chemoattr. source	[8]
b_0	$1 \cdot 10^{-2}/V_B\ [1/Vol]$	Half-saturation in (1-D)	[8]
K	$1 \cdot 10^{-10}\ \left[m^2/sec\right]$	Motility	estimate [1]
χ	$0.5 - 0.05\ \left[m^2/sec\right]$	Chemotaxis coefficient	[8]
μ	10^{-8} - $10^{-9}\ \left[m^2/sec\right]$	Macroph. death rate	estimate [8]

3. **Non-dimensional system.** Assuming to stay in a two-dimensional space, it is useful to re-write our system in a non-dimensional form.

We know that $x, y \in [0, L]$ and $t \in [0, T]$. We introduce

$$\xi = \frac{x}{L};\ \psi = \frac{y}{L};\ \tau = \frac{t}{\zeta}, \tag{10}$$

where we choose $\zeta = 1/\Gamma_C\ [sec]$. The derivatives are as follows:

$$\frac{\partial}{\partial t} = \frac{1}{\zeta}\frac{\partial}{\partial \tau};\ \frac{\partial}{\partial x} = \frac{1}{L}\frac{\partial}{\partial \xi};\ \frac{\partial}{\partial y} = \frac{1}{L}\frac{\partial}{\partial \psi};\ \frac{\partial^2}{\partial x^2} = \frac{1}{L^2}\frac{\partial^2}{\partial \xi^2};\ \frac{\partial^2}{\partial y^2} = \frac{1}{L^2}\frac{\partial^2}{\partial \psi^2}. \tag{11}$$

B and M are the number of bacteria in a unitary volume and the number of macrophages in a unitary volume respectively. Then, to obtain non-dimensional unknowns, we put

$$\hat{B} = BV_B,\ \hat{M} = MV_M,\ \hat{C} = \frac{\Gamma_c}{\sigma_B}C,\ \hat{v} = -\hat{K}\left(\hat{\nabla}\cdot\hat{B} + \hat{\nabla}\cdot\hat{M}\right); \tag{12}$$

where V_B and V_M are the volume of a single bacterium and macrophage, respectively. The non-dimensional constants are

$$\hat{D}_B = \frac{\zeta}{L^2}D_B,\ \hat{D}_M = \frac{\zeta}{L^2}D_M,\ \hat{\alpha} = \zeta\alpha,\ \hat{\lambda} = \frac{\lambda\zeta}{V_M},\ \hat{\mu} = \zeta\mu,\ \hat{K} = \zeta\frac{K}{L^2},$$
$$\hat{b_0} = b_0V_B,\ \hat{\chi} = \frac{\sigma_B\zeta}{\Gamma_C L^2}\chi,\ \zeta = 1/\Gamma_C\ \hat{D}_C = \frac{\zeta}{L^2}D_C,\ \hat{\Gamma}_M = \zeta\frac{\Gamma_M}{V_M}. \tag{13}$$

Therefore, using equations (1), (2), (3) and (8), the **non-dimensional** system is given by

$$\hat{C}_\tau - \hat{D}_C\Delta\hat{C} = \frac{\hat{B}}{\hat{B}+\hat{b_0}} - \hat{C} - \hat{\Gamma}_M\hat{M}\hat{C}, \tag{14}$$
$$\hat{B}_\tau - \hat{D}_B\Delta\hat{B} = \hat{K}\nabla\cdot\left(\hat{B}\nabla\hat{B}\right) + \hat{K}\nabla\cdot\left(\hat{B}\nabla\hat{M}\right) + \hat{\alpha}\hat{B} - \hat{\lambda}\hat{B}\hat{M}, \tag{15}$$
$$\hat{M}_\tau - \hat{D}_M\Delta\hat{M} = \hat{K}\nabla\cdot\left(\hat{M}\nabla\hat{B}\right) + \hat{K}\nabla\cdot\left(\hat{M}\nabla\hat{M}\right) - \hat{\chi}\nabla\cdot\left(\hat{M}\nabla\hat{C}\right) - \hat{\mu}\hat{M}. \tag{16}$$

The **boundary conditions** are

$$\mathbf{n}\cdot\nabla\hat{B} = \mathbf{n}\cdot\nabla\hat{M} = \mathbf{n}\cdot\nabla\hat{C} = 0,\ at\ \partial\Omega\times(0,T_M); \tag{17}$$

and the **initial conditions** are given by the nonnegative functions

$$\hat{B}(0,\xi,\psi) = \hat{B}_0(\xi,\psi),\ \hat{M}(0,\xi,\psi) = \hat{M}_0(\xi,\psi),\ \hat{C}(0,\xi,\psi) = \hat{C}_0(\xi,\psi). \tag{18}$$

A list of non-dimensional parameters is given in table 2.

Remark 2. From now on, we will use always the non dimensional system; non-dimensional variables will be directly referred to as (x,y,t), and non-dimensional constants, previously denoted by "hat" ($\hat{}$) quantities, will be indicated without "hat", unless a different notation is explicitly introduced.

So, our system in the non-dimensional form rewrites

$$B_t + \nabla\cdot(vB) - D_B\Delta B = \alpha B - \lambda BM, \tag{19}$$
$$M_t + \nabla\cdot(vM) + \nabla\cdot(\chi M\nabla C) - D_M\Delta M = -\mu M, \tag{20}$$
$$C_t - D_C\Delta C = \frac{B}{B+b_0} - C - \Gamma_M MC, \tag{21}$$

where

$$v = -K\left(\nabla B + \nabla M\right). \tag{22}$$

The **boundary conditions** are

$$\mathbf{n}\cdot\nabla B = \mathbf{n}\cdot\nabla M = \mathbf{n}\cdot\nabla C = 0,\ at\ \partial\Omega\times(0,T_M), \tag{23}$$

and the **initial conditions** are

$$B_0(x,y)\geq 0,\ M_0(x,y)\geq 0,\ C_0(x,y)\geq 0. \tag{24}$$

TABLE 2. Non-dimensional parameters table

Non-dimensional parameters	value
$\hat{D}_B = \frac{\zeta}{L^2} D_B$	$10^{-3} - 10^{-4}$
$\hat{D}_M = \frac{\zeta}{L^2} D_M$	10^{-1}
$\hat{D}_C = \frac{\zeta}{L^2} D_C$	10
$\hat{\alpha} = \zeta \alpha$	500
$\hat{K} = \zeta \frac{K}{L^2}$	1
$\hat{b_0} = b_0 V_B$	10^{-2}
$\hat{\chi} = \frac{\sigma_B \zeta}{\Gamma_C L^2} \chi$	$5 - 50$
$\hat{\mu} = \zeta \mu$	$0.1 - 1$
$\hat{\Gamma}_M = \zeta \frac{\Gamma_M}{V_M}$	10^{-9}

4. **Discussion on linear stability analysis in 1-D.** In this section, we study the linear approximation of our system in one-dimension using the non-dimensional system. As first step, we find homogeneous steady state solutions. Then, we study their stability, and, finally, we analyze what happens to the linear unstable area using the nonlinear system.

Here, we assume to have an immune system able to maintain its efficiency for a long time period. This means that there exists an equilibrium between the macrophage death and birth. Since we have no-flux of matter from the boundaries, we choose $\mu = 0$ to maintain constant the number of macrophages.

The homogeneous steady state is indicated by $\left(\bar{B}, \bar{M}, \bar{C}\right)$. Then, using equations (19)-(24) and assuming $\mu = 0$, we obtain:

$$\bar{B},\ \bar{M} = \frac{\alpha}{\lambda},\ \bar{C} = \left(\frac{\bar{B}}{\bar{B} + b_0}\right) \frac{1}{1 + \Gamma_M \bar{M}}. \tag{25}$$

Thus, we indicate the homogeneous solutions by

$$\begin{pmatrix} B(t) \\ M(t) \\ C(t) \end{pmatrix} = \begin{pmatrix} \bar{B} + b(t) \\ \bar{M} + m(t) \\ \bar{C} + c(t) \end{pmatrix}$$

where $(b(t), m(t), c(t))$ represent the homogeneous perturbations. Then, equations of time evolution for homogeneous solutions are

$$\begin{aligned} B_t &= \alpha B - \lambda B M; \\ M_t &= 0; \\ C_t &= \frac{B}{B + b_0} - C\left(1 + \Gamma_M M\right). \end{aligned} \tag{26}$$

Taking into account that $M = \bar{M} + m$ and $\bar{M} = \alpha/\lambda$, we find out

$$\begin{aligned} B(t) &= B_0 e^{-\lambda m t}; \\ M(t) &= M_0; \\ C(t) &\leq \frac{1}{(1+\Gamma_M M_0)} + e^{-(1+\Gamma_M M_0)t}. \end{aligned} \tag{27}$$

If $m > 0$, B is decreasing exponentially; if $m < 0$, B increases exponentially. Also $C(t)$ is upper limited, see eq. (27).

This means that bacteria are contained if $\bar{M}+m > \frac{\alpha}{\lambda}$, otherwise ($m < 0$) bacteria increase exponentially.

4.1. **Non-homogeneous perturbations.** Now, we want to see what happen considering non-homogeneous perturbations. In this case, small perturbations are ϵ, δ and γ, such that: $B = \bar{B} + \epsilon$, $M = \bar{M} + \delta$ and $C = \bar{C} + \gamma$. Linearizing our system about the homogeneous steady state, we find out

$$\begin{aligned} &\epsilon_t - \left(K\bar{B} + D_B\right)\epsilon_{xx} - K\bar{B}\delta_{xx} = -\lambda\bar{B}\delta, \\ &\delta_t - K\bar{M}\epsilon_{xx} - \left(K\bar{M} + D_M\right)\delta_{xx} + \chi\bar{M}\gamma_{xx} = 0, \\ &\gamma_t - D_C\gamma_{xx} = \omega_B\epsilon - \gamma; \end{aligned} \tag{28}$$

where $\omega_B = \dfrac{b_0}{(\bar{B}+b_0)^2}$. Notice that we used the approximation $(1+\Gamma_M M) \approx 1$, see table 2.

4.2. **Linear stability.** We now look for solutions of (28) in the form

$$\epsilon = b_n \cdot e^{\Lambda t}\cos(n\pi x),\ \ \delta = m_n \cdot e^{\Lambda t}\cos(n\pi x),\ \ \gamma = c_n \cdot e^{\Lambda t}\cos(n\pi x), \tag{29}$$

where n indicates the number of the mode.

Substituting (29) in the system (28), and indicating the solutions by the vector $w = (\epsilon, \delta, \gamma)$, we can write $Qw = 0$, where the matrix Q is

$$Q = \begin{pmatrix} -n^2\pi^2\left(K\bar{B} + D_B\right) & -\left(\lambda\bar{B} + n^2\pi^2 K\bar{B}\right) & 0 \\ -n^2\pi^2 K\bar{M} & -n^2\pi^2\left(K\bar{M} + D_M\right) & n^2\pi^2\chi\bar{M} \\ \omega_B & 0 & -\left(n^2\pi^2 D_C + 1\right) \end{pmatrix}$$

The characteristic polynomial of Q is

$$P(\Lambda) = \Lambda^3 + a_1\Lambda^2 + a_2\Lambda + a_3 = 0. \tag{30}$$

If $n = 0$, the eigenvalues are: $(0, 0, -1)$, we have constant solutions for $\Lambda = 0$ and a negative exponential for $\Lambda = -1$. It is stable for null-average perturbations.

Proposition 1. *There exists a positive value $B_0 \approx 8 \cdot 10^{-6}$, such that if $\bar{B} < B_0$, then the solutions of (28) are linearly stable for $n \geq 1$. If $\bar{B} > B_0$, there exists a critical index $n(\bar{B})$, such that the n-mode n is linearly unstable for $1 \leq n \leq n(\bar{B})$. The other modes are always stable. The critical index $n(\bar{B})$ is monotone increasing with respect to $\bar{B}$, and it tends to a value $n_1 \approx 22.5$ as $\bar{B} \to 1$.*

Proof. We assume $p = n^2\pi^2 > 0$, then we have

$$a_1 = 1 + \left(D_B + D_C + D_M + K\bar{B} + K\frac{\alpha}{\lambda}\right)p \tag{31}$$

$$\begin{aligned} a_2 = &\left(D_B + D_M + K\bar{B}\,(1-\alpha) + K\frac{\alpha}{\lambda}\right)p \\ &+ \left(D_B D_C + D_B D_M + D_C D_M + K D_C \bar{B}\right. \\ &\left. + K D_M \bar{B} + K\frac{\alpha}{\lambda}\,(D_B + D_C)\right)p^2, \end{aligned} \tag{32}$$

$$\begin{aligned} a_3 = &\left(\frac{b_0}{\bar{B}+b_0}\chi\alpha\bar{B} - K\alpha\bar{B}\right)p + \left(K\frac{\alpha}{\lambda}\left(D_B + \frac{b_0}{\bar{B}+b_0}\chi\bar{B}\right) - K\alpha D_C\bar{B}\right. \\ &\left. + K D_M\bar{B} + D_B D_M\right)p^2 + \left(D_B D_C D_M + K D_C D_M \bar{B} + K D_C D_B\frac{\alpha}{\lambda}\right)p^3. \end{aligned} \tag{33}$$

These solutions are stable if all roots Λ of the characteristic polynomial (30) lie in the left-hand complex plane: $Re\Lambda < 0$. To this goal, we use the Routh-Hurwitz conditions [14]

$$a_1 > 0,\ a_3 > 0,\ a_1 a_2 - a_3 > 0. \tag{34}$$

4.2.1. $a_1 > 0$. We have $a_1 = 1 + n^2\pi^2\left(D_B + D_C + D_M + K\bar{B} + K\bar{M}\right) > 0$, then, the first condition of (34) is always satisfied.

4.2.2. $a_1 a_2 - a_3 > 0$. Here, we want to see when $a_1 a_2 - a_3 > 0$ is satisfied. Using equations (31), (32) and (33), and simplifying them, we find

$$\begin{aligned} a_1 a_2 - a_3 \approx &-\alpha\bar{B}\chi p + \left(D_M\left(2D_C - K\frac{\alpha}{\lambda}\right) + K D_C\alpha\bar{B}\right)p^2 \\ &+ D_M D_C\,(D_C - D_B)\,p^3. \end{aligned} \tag{35}$$

Taking into account parameter values in table 2, $\lambda \approx 10^4$, and $p = n^2\pi^2$ ($n = 1, 2...$), we obtain that the (35) is greater than zero for any p, making the realistic approximation that $\bar{B} < 10^{-2}$.

4.2.3. $a_3 > 0$. To satisfy $a_3 > 0$, we write

$$a_3 = \beta_1 + \beta_2 p + \beta_3 p^2, \tag{36}$$

where

$$\begin{aligned} \beta_1 &= \alpha\bar{B}\left(\frac{b_0}{b_0+\bar{B}}\chi - K\right), \\ \beta_2 &= D_M\left(D_B + K\bar{B}\right) + K\frac{\alpha}{\lambda}\left(D_M + \frac{b_0}{b_0+\bar{B}}\chi\bar{B}\right) - K\alpha D_C\bar{B}, \\ \beta_3 &= D_C D_M\left(D_B + K\bar{B}\right) + D_B D_C K\frac{\alpha}{\lambda}. \end{aligned} \tag{37}$$

Now, we search for the positivity region of a_3. First, we find out

$$\beta_1 > 0,\ \beta_3 > 0. \tag{38}$$

The two roots of eq. (36) are

$$p_\pm(\bar{B}) = \frac{-\beta_2 \pm \sqrt{\beta_2^2 - 4\beta_1\beta_3}}{2\beta_3}. \tag{39}$$

Calling $r(\bar{B}) = \beta_2^2 - 4\beta_1\beta_3$, we obtain that $r(\bar{B}) < 0$ (figure 1), for

$$B_1 < \bar{B} < B_0;\ B_1 = 1\cdot 10^{-7},\ B_0 = 8\cdot 10^{-6}.$$

Thus,

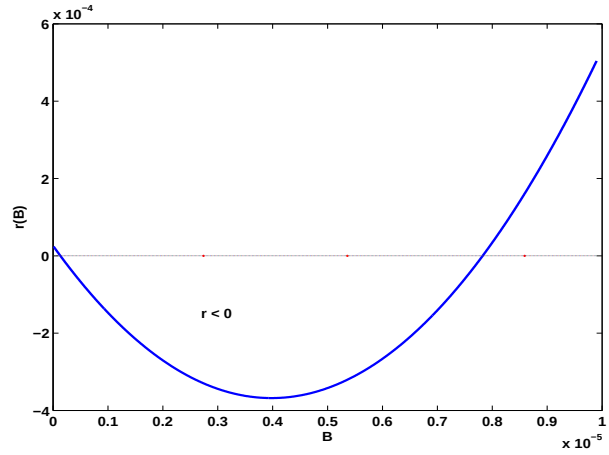

FIGURE 1. Region in which $r(\bar{B})$ assume negative values.

1. If $r < 0$ we find imaginary roots, then $a_3 > 0$ always.
2. If $r > 0$, we have two regions: $\bar{B} < B_1$ and $\bar{B} > B_0$. We consider only $\bar{B} > B_0$, and $p = n^2\pi^2 > p_+$, because in the other cases $n < 1$. Then, the function $p_+(\bar{B})$ describe the positivity of a_3: if $p > p_+$, $a_3 > 0$, otherwise $a_3 < 0$, see figure 2.

Thus, we have obtained an unstable region ($a_3 < 0$) defined by $p_+(\bar{B})$ and for $\bar{B} > B_0$. Also we observed that for $\bar{B} \to 1$, $p_+ \to \alpha D_c = 5000$, this means that $n_+ \approx 22.5$. Thus we can conclude that for $n \geq 23$ the region is stable for any $\bar{B}$. □

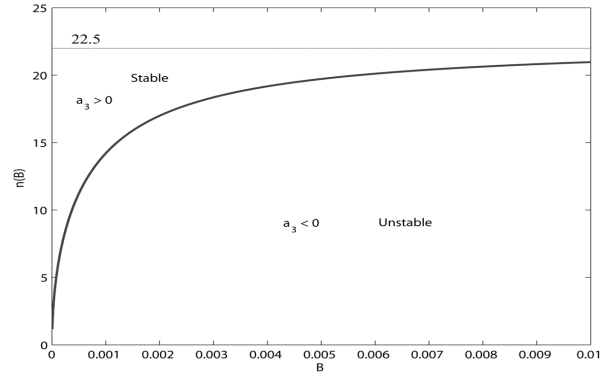

FIGURE 2. Behavior of $n_+(\bar{B})$; ($p_+ = n_+^2\pi^2$), which defines the positivity of a_3.

4.3. **Simulations of small perturbations.** Here, we consider perturbations of the following homogeneous solutions: $\bar{B} = 0$, $\bar{C} = 0$ and three different $\bar{M}$:

$1)\bar{M} \approx 10\dfrac{\alpha}{\lambda}$, $2)\bar{M} \approx 0.1\dfrac{\alpha}{\lambda}$ and $3)\bar{M} \approx \dfrac{\alpha}{\lambda}$.

The perturbation of bacteria (ϵ) is a distribution of about 100 bacteria in the center of the domain, the other perturbations are $\delta = 0$ and $\gamma = \epsilon/(\epsilon + b_0)$. Numerical simulations are realized on the non linear system (19)-(24), using the numerical approximations described in section 5.

The case 1 ($\bar{M} \approx 10\dfrac{\alpha}{\lambda}$) is on the left side of figure 3, where bacteria are cleared as expected. The case 2 ($\bar{M} \approx 0.1\dfrac{\alpha}{\lambda}$) is on the right side of of figure 3: here, we observe a bacteria growth. The third case ($\bar{M} \approx \dfrac{\alpha}{\lambda}$), is in figure 4. This case

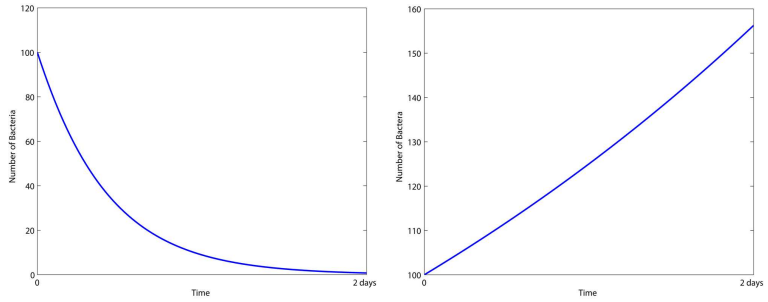

FIGURE 3. Left: number of bacteria with $\bar{M} \approx 10\dfrac{\alpha}{\lambda}$. Right: number of bacteria with $\bar{M} \approx 0.1\dfrac{\alpha}{\lambda}$.

presents an interesting aspect: if the perturbation ϵ is homogeneously distributed in space, we observe that the number of bacteria remains the same (see left side of figure 4); if the perturbation is non-homogeneous, and concentrated in the center of the domain, we have a mild reduction of bacteria, see the right side of figure 4. This different behavior implies that the geometry of the initial distribution of bacteria can influence their evolution.

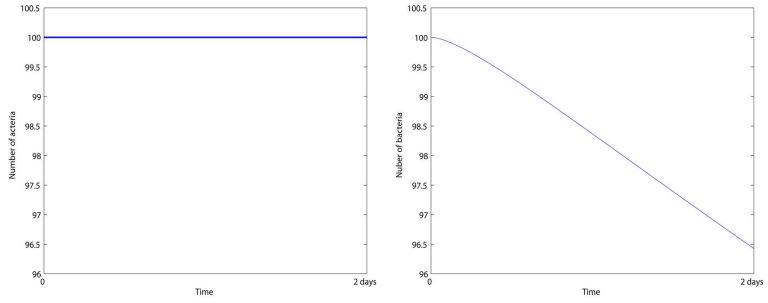

FIGURE 4. Left side figure: number of bacteria with initial perturbation homogeneous. Right side figure: bacteria concentrated in the middle of domain.

4.4. **Long time behavior of linear instability.** In section 4, we observed that for $\bar{B} > B_0$ solutions are linearly unstable. In this paragraph, we study the influence of non-linear terms on the linear instability. Using the non-linear system (19)-(24), we choose as initial conditions $M(0) = \bar{M} = \dfrac{\alpha}{\lambda}$, $C(0) = \dfrac{B(0)}{b_0 + B(0)}$, and two different initial conditions for bacteria:

1. $B(0) = B_a = \bar{B}_a + \epsilon(0)$, where $B_a = 10^{-10} < B_0$ and ϵ is a small perturbation.
2. $B(0) = B_b = \bar{B}_b + \epsilon(0)$, where $\bar{B}_b = 10^{-5} > B_0$.

The initial bacteria perturbation $\epsilon(0)$ is on the left side of figure 5. Simulating ten years evolution of these two cases, by an implicit scheme, we obtain that the perturbation of B_a is more quickly diffused, while perturbation of B_b (linearly unstable) does not blow up, and it remains contained. Both simulations are shown on the right side of figure 5.

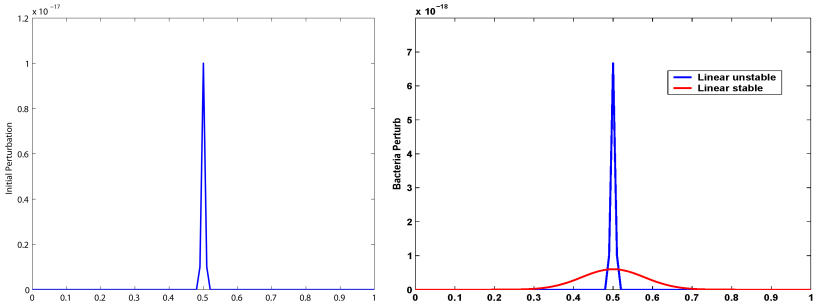

FIGURE 5. Left: initial perturbation of bacteria is on the left. Right: B_a (in red) and B_b (in blue) after 10 years simulations.

To the light of these results, we can observe that whereas there is linear stability, perturbation tends to flatten out to its initial value; and whereas there is linear instability, perturbation tends to hold its shape. This is due to the non linear damping effect which contrasts the linear instability effect. For these reasons, results agree with our linear analysis.

5. **Numerical schemes.** To solve our model we make use of Implicit-Explicit (IMEX) schemes ([20], [3]). For the sake of simplicity, we show the one-dimensional scheme, which can be easily extended in two-dimensions:

5.1. **IMEX scheme.** We represent the system as

$$U_t = H(U) + G(U), \tag{40}$$

where

$$U = \begin{pmatrix} C \\ B \\ M \end{pmatrix},$$

$$H(U) = \begin{pmatrix} \dfrac{B}{B + b_0} - C - \Gamma_M MC \\ (KB_x B + KM_x B)_x + \alpha B - \lambda BM \\ (KMB_x + KMM_x - \chi C_x M)_x - \mu M \end{pmatrix},$$

and

$$G(U) = \begin{pmatrix} D_C C_{xx} \\ D_B B_{xx} \\ D_M M_{xx} \end{pmatrix}.$$

We integrate explicitly $H(U)$, while $G(U)$ is a stiff term which will be integrated implicitly to avoid excessively small time steps.

A general IMEX-DIRK Runge-Kutta scheme is given by, for $t = n\Delta t$

$$u^{(i)} = u^n + \Delta t \sum_{k=1}^{i-1} \tilde{a}_{ik} H(u^{(k)}) + \Delta t \sum_{k=1}^{i} a_{ik} G(u^{(k)}),\ i = 1, ...\nu \tag{41}$$

$$u^{n+1} = u^n + \Delta t \sum_{i=1}^{\nu} \tilde{\omega}_i H(u^{(i)}) + \Delta t \sum_{i=1}^{\nu} \omega_i G(u^{(i)}). \tag{42}$$

The matrices $\tilde{A} = (\tilde{a}_{ik})$, where $\tilde{a}_{ik} = 0$ for $j \geq i$ and $A = (a_{ik})$ are $\nu \times \nu$ matrices such that the resulting scheme is explicit in H and implicit in G. The DIRK formulation requires $a_{ik} = 0$ for $j > i$ [3].

Now, we write H and G in the discrete numerical form. To this goal, we develop each term in the following way (where $n = 1, ..., N$ is the time index and $j = 1, ..., J$ is the space index):

$$(H_1)_j^n = \frac{B_j^n}{B_j^n + b_0} - C_j^n - \Gamma_M M_j^n C_j^n, \tag{43}$$

$$\begin{aligned} &(H_2)_j^n \\ &= \frac{K}{2\Delta x^2}\left(\left(B_j^n + B_{j+1}^n\right)\left(B_{j+1}^n - B_j^n\right) - \left(B_{j-1}^n + B_j^n\right)\left(B_j^n - B_{j-1}^n\right)\right) \\ &+ \frac{K}{2\Delta x^2}\left(\left(B_j^n + B_{j+1}^n\right)\left(M_{j+1}^n - M_j^n\right) - \left(B_{j-1}^n + B_j^n\right)\left(M_j^n - M_{j-1}^n\right)\right) \\ &+ \alpha B_j^n - \lambda B_j^n M_j^n; \end{aligned} \tag{44}$$

$$\begin{aligned} &(H_3)_j^n \\ &= \frac{K}{2\Delta x^2}\left(\left(M_j^n + M_{j+1}^n\right)\left(B_{j+1}^n - B_j^n\right) - \left(M_{j-1}^n + M_j^n\right)\left(B_j^n - B_{j-1}^n\right)\right) \\ &+ \frac{K}{2\Delta x^2}\left(\left(M_j^n + M_{j+1}^n\right)\left(M_{j+1}^n - M_j^n\right) - \left(M_{j-1}^n + M_j^n\right)\left(M_j^n - M_{j-1}^n\right)\right) \\ &- \frac{\chi}{2\Delta x^2}\left(\left(M_j^n + M_{j+1}^n\right)\left(C_{j+1}^n - C_j^n\right) - \left(M_{j-1}^n + M_j^n\right)\left(C_j^n - C_{j-1}^n\right)\right) \\ &- \mu M_j^n. \end{aligned} \tag{45}$$

For G, we use a three-points centered approximation

$$(G_1)_j^n = \frac{D_C}{\Delta x^2}\left(C_{j+1}^n - 2C_j^n + C_{j-1}^n\right), \tag{46}$$

$$(G_2)_j^n = \frac{D_B}{\Delta x^2}\left(B_{j+1}^n - 2B_j^n + B_{j-1}^n\right), \tag{47}$$

$$(G_3)_j^n = \frac{D_M}{\Delta x^2}\left(M_{j+1}^n - 2M_j^n + M_{j-1}^n\right). \tag{48}$$

5.2. **Numerical simulations 1-D.** Here, we present bacteria evolution for different macrophage distribution. Assuming an initial infection of 50 bacteria, we present three simulations. In the first one, we suppose to have 170 macrophages distributed in the area, in the second one 430 and in the third one 690. In each one

of these cases, we adopt different values of the efficiency parameter λ, in order to estimate the efficiency required to contain or not the infection.

1. **Case I: 170 macrophages**. The evolution of the number of bacteria with different λ values is in figure 6. There, macrophages are able to contain infection if $\lambda > \lambda_c = 3 \cdot 10^4$.
2. **Case II:** 430 **macrophages** The evolution of the number of bacteria with different λ values is in figure 7. In this second case, macrophages are able to contain infection if $\lambda > \lambda_c = 1.1 \cdot 10^4$.
3. **Case III:** 690 **macrophages** The evolution of the number of bacteria with different λ values is in figure 8. In this third case, macrophages are able to contain infection if $\lambda > \lambda_c = 6.6 \cdot 10^3$.

5.3. **Discussion.** It is interesting to compare these simulations with the results obtained in section 4 with homogeneous solutions. There, $\bar{M} \approx \frac{\alpha}{\lambda}$, is the boundary between bacteria contained or not.

Here, in the case I (170 macrophages), we have $\alpha/\lambda_c = 0.0167$ and $\bar{M}_I = 0.0170$, i.e. numerical simulations give us a result in a good agreemet with the analysis in section 4. Similar results are also in the case II where $\alpha/\lambda_c \approx 0.045$ and $\bar{M}_I = 0.043$, and in the case III where $\alpha/\lambda_c \approx 0.075$ and $\bar{M}_I = 0.069$.

We can conclude that, both in the homogeneous solutions and full model simulations, we obtained the same order of magnitude for the boundary value of λ.

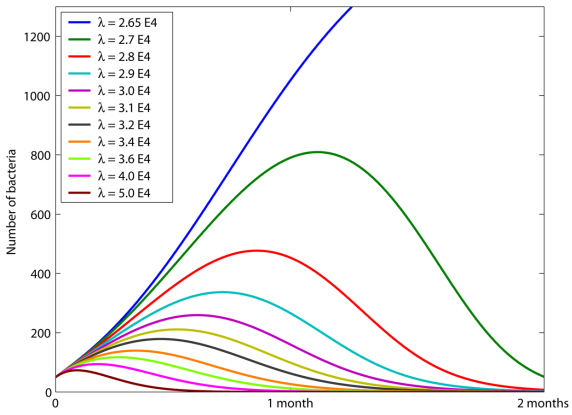

FIGURE 6. Case I. Number of bacteria with different values of λ and with 170 macrophages initially present.

6. **Simulations in the two-dimensional case.** In this section we use the pressure model in two-dimensions. In the first part of the section we simulate a case in which bacteria prevail, then, a case in which bacteria are contained. Equations of the model are given by (19)-(24).

6.1. **Numerical simulations.** We assume to have initially about 10^5 macrophages randomly distributed in an area of 1 $[dm^2]$, and in the middle of this area we assume to have an initial infection of 400 bacteria. Under these assumptions we have simulated the evolution of infection in the first two months, using the parameters in table 3 below

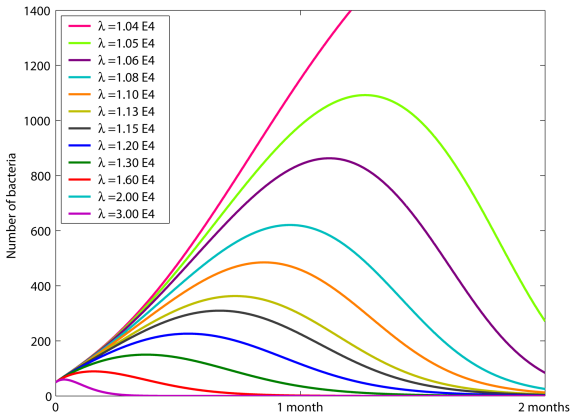

FIGURE 7. Number of bacteria with different values of λ and with 430 macrophages initially present.

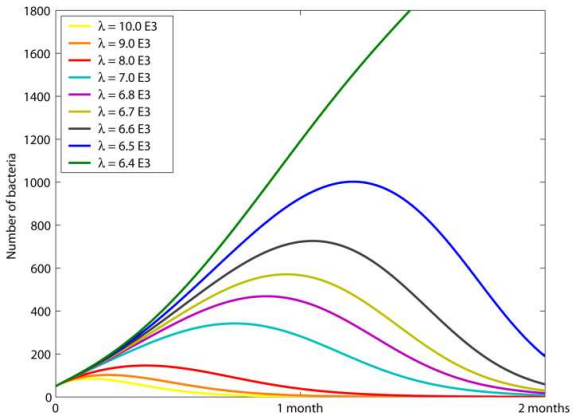

FIGURE 8. Number of bacteria with different values of λ, with 690 macrophages.

6.1.1. *Bacteria prevailing.* In the first case we use the non-dimensional value $\lambda = 4.5 \cdot 10^5$. It gives origin to an uncontrolled growth of bacteria. Here, we present the behavior of bacterium and macrophage concentration in the first two months. In figure 9 we can see their initial distribution, in figure 10 we can see their distribution after 1 month and in figure 11 after 2 months.

In figure 11 we can observe the clustering of macrophages in the middle of region, due to the great infection located there, which attracts macrophages by chemotaxis. Finally, we show the number of bacteria evolution in the first two months in figure 12.

6.1.2. *Bacteria contained.* Here, we present simulations describing a case in which bacteria are contained by macrophages. We use the non-dimensional value $\hat{\lambda} = 9.5 \cdot 10^5$. In figure 13 we can see their initial distribution, in figure 14 we can see their distribution after 1 month and in figure 15 after 2 months. Finally, in figure 16 we show the number of bacteria in the first two months.

TABLE 3. Parameters (dimensional) table

Parameter	Indications	value
V_M	Macrophage volume	$10^{-10}\ [m^2]$
V_B	Bacterium volume	$10^{-12}\ [m^2]$
D_M	Macrophage diffusion	$10^{-11}\ [m^2/sec]$
D_B	Bacteria diffusion	$10^{-13}\ [m^2/sec]$
D_C	Chemoattractant diffusion	$10^{-10}\ [m^2/sec]$
χ	Chemotaxis coefficient	$100\ [m^2/sec]$
μ	Macrophage death rate	$10^{-7}\ [1/sec]$
α	Bact. (double every 38 hours)	$5 \cdot 10^{-6}\ [1/sec]$
Γ_M	Macrophage death rate	$10^{-22}\ [1/sec]$
K	Transport coefficient	$10^{-10}\ [m^2/sec]$

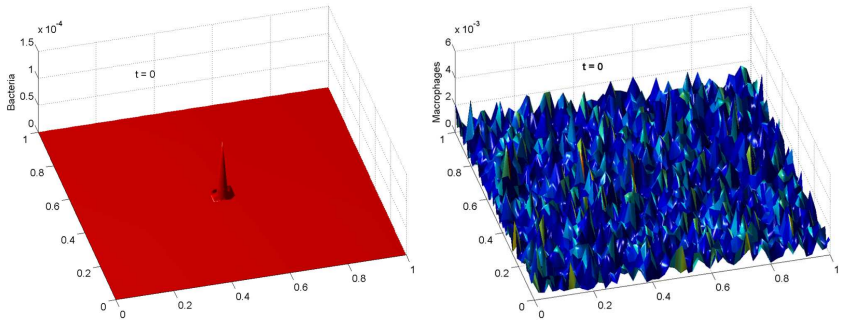

FIGURE 9. Bacterium (left) and macrophage (right) distribution at initial instant.

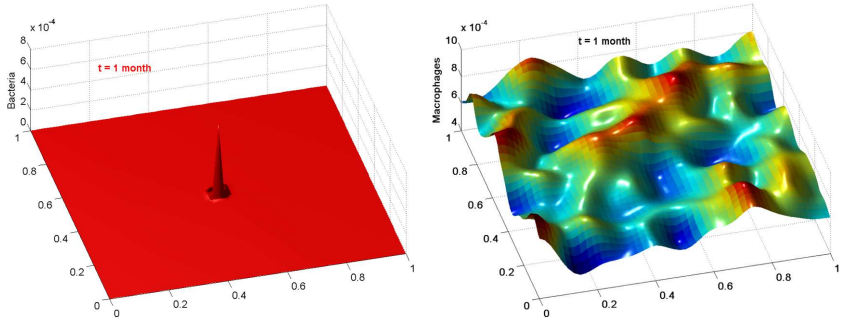

FIGURE 10. Bacterium (left) and macrophage (right) distribution after 1 month.

6.1.3. *Comparison with different efficiency coefficients.* In figure 17 we compare the behavior of the infection (number of bacteria) varying the coefficient λ from $5 \cdot 10^5$, case in which bacteria increases their number exponentially, and $\lambda = 9.5 \cdot 10^5$, case in which infection is controlled by innate immune response. It is evident that for $\lambda \leq 6.3 \cdot 10^5$ we have an uncontrolled growth.

6.2. **Variation of immune response.** In this section we want to present a couple of examples in which the immune response can change with time. As first example,

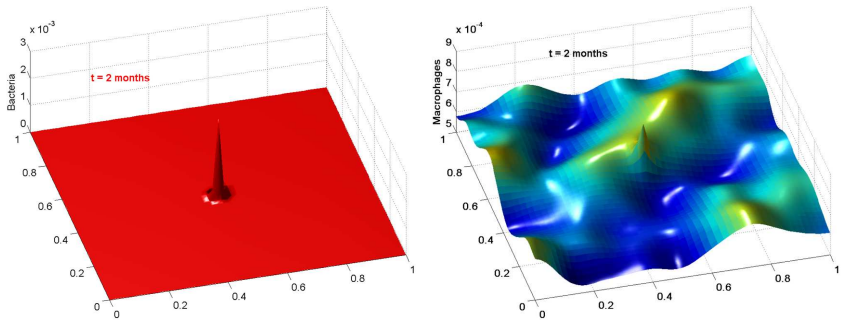

FIGURE 11. Bacterium (left) and macrophage (right) distribution after 2 months.

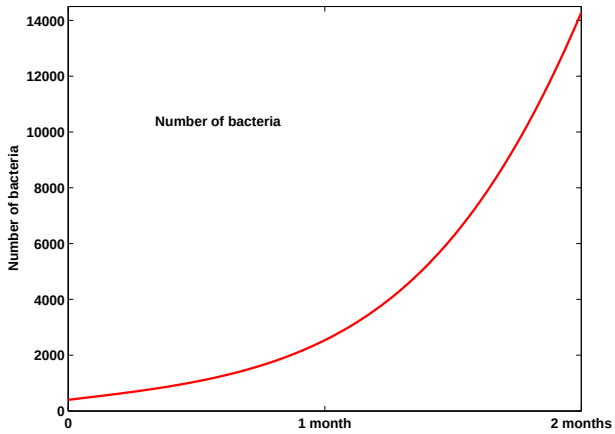

FIGURE 12. Number of bacteria growth in 2 months. Case in which bacteria are prevailing with $\lambda = 4.5 \cdot 10^5$.

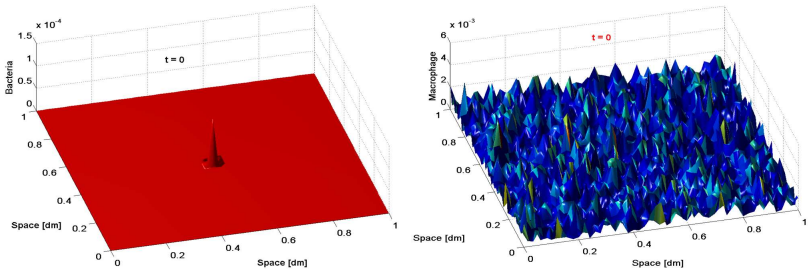

FIGURE 13. Bacterium (left) and macrophage (right) distribution at initial instant.

we want to simulate a sort of reactivation of infection. It can be due to two different causes: the first one is a diminishing number of macrophages; the second one is a diminishing efficiency to kill bacteria. These two causes are simulated in section 6.2.1. As second example, we want to represent a strengthening of immune system, a sort of simplified adaptive immune response. To make so, we assume that after

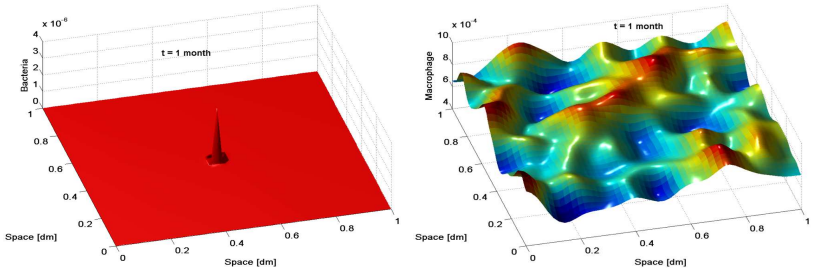

FIGURE 14. Bacterium (left) and macrophage (right) distribution after 1 month.

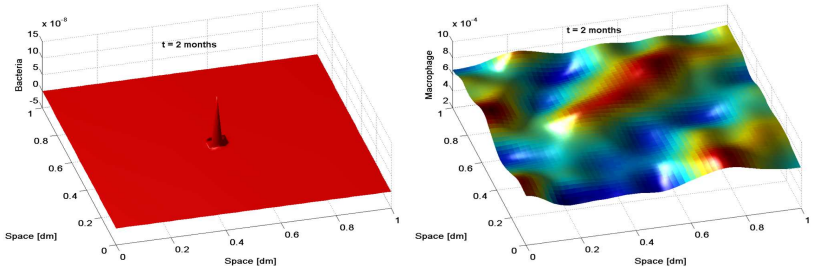

FIGURE 15. Bacterium (left) and macrophage (right) distribution after 2 months.

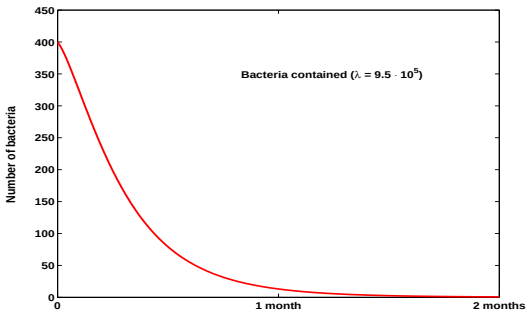

FIGURE 16. Number of bacteria growth in 2 months. Case with $\lambda = 9.5 \cdot 10^5$, bacteria contained

three weeks, the efficiency of immune system (λ coefficient) increases its value of three times, and the macrophages death rate (μ) diminishes.

6.2.1. *Case I: Reactivation.*

a) Here, we assume to have a constant non-dimensional macrophage death rate $\mu = 10$. We suppose, also, that there is no incoming macrophages from outside, then the number of macrophages is diminishing, weakening the immune system. Choosing $\lambda = 9.5 \cdot 10^5$ we have that initially macrophages contain infection. But, after about six months, when the number of macrophages is 50% the infection of bacteria arises again. This way, we want to represent a sort of simplified reactivation, in a brief time with respect to reality (years). In figure 18 we can see the concentration of bacteria at several time points.

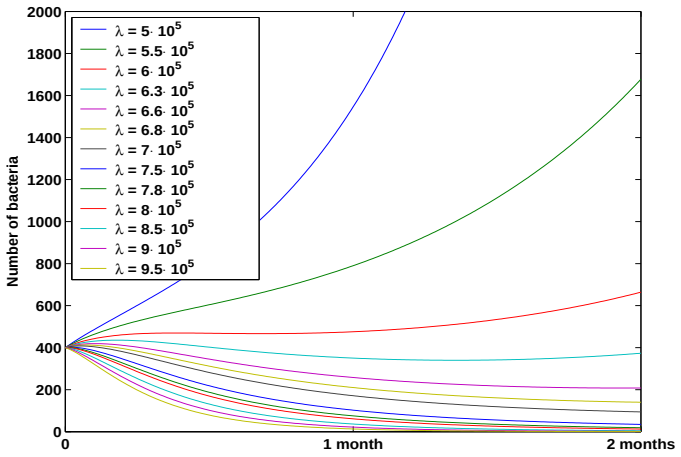

FIGURE 17. Comparison among number of bacteria with different values of λ coefficient.

Then, in figure 19 is shown the variation of the number of bacteria (upper) and the number of macrophages (lower).

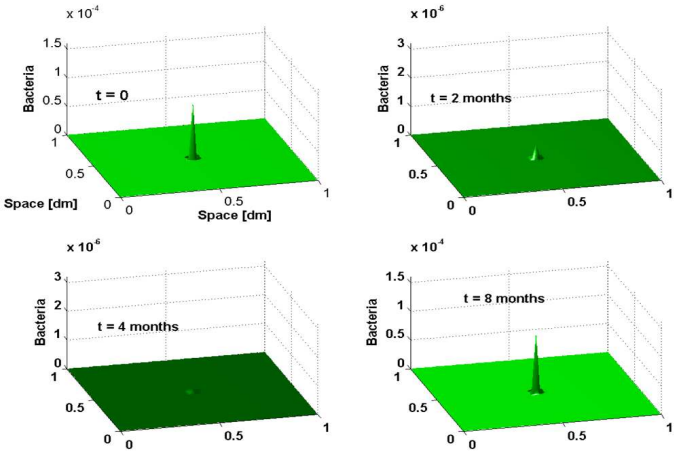

FIGURE 18. Bacteria concentration at initial time, after 2, 4 and 8 months.

b) Here, we imagine a lower efficiency of immune system: $\lambda = \lambda(t)$ is a function of time, it varies linearly from $9 \cdot 10^5$ (at $t = 0$) to $\lambda = 4 \cdot 10^5$ (for $t = 8$ months). The death rate lower than the previous case, it is $\mu = 3 \cdot 10^5$. Under these assumptions we obtain the behavior of bacteria concentration in figure 20 and the evolution of the number of bacteria in figure 21. In this case the number of macrophages diminish about 15% in eight months.

6.2.2. *Case II: Strengthening of immune response.* Here, we assume that after three weeks the non-dimensional coefficient λ increases, and the death rate of macrophages μ (non-dimensional) becomes smaller. This means that after three weeks the immune response improve (adaptive immune response) and the macrophage death rate

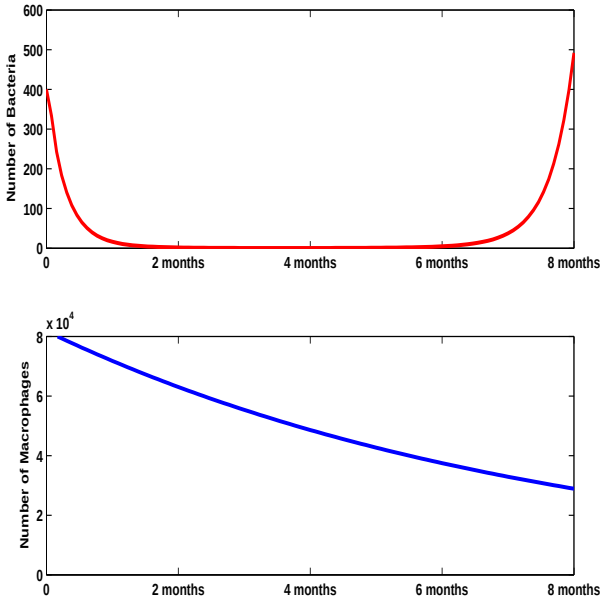

FIGURE 19. Number of bacteria (upper) and number of macrophages (lower) in the first 8 months.

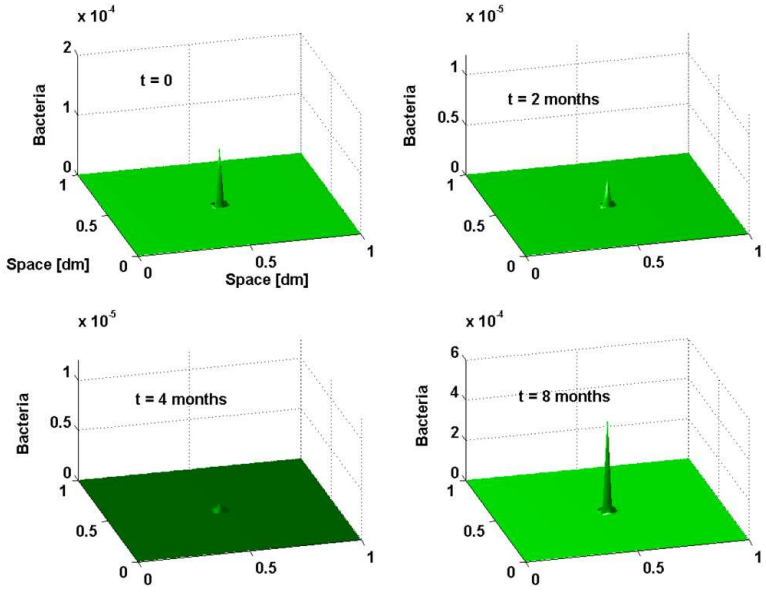

FIGURE 20. Bacteria concentration at initial time, after 2, 4 and 8 months.

diminishes for their improved effectiveness. Using $\mu = 3$ in the first three weeks, after that $\mu = 0.5$. While $\lambda = \lambda_1$ in the first three weeks, then λ increases linearly to the value of λ_2 in the next 9 weeks, then it is $\lambda = \lambda_2$ up to eighth month. We choose four cases: a) $\lambda_1 = 3 \cdot 10^5$, $\lambda_2 = 1 \cdot 10^6$; b) $\lambda_1 = 3 \cdot 10^5$, $\lambda_2 = 8 \cdot 10^5$; c)

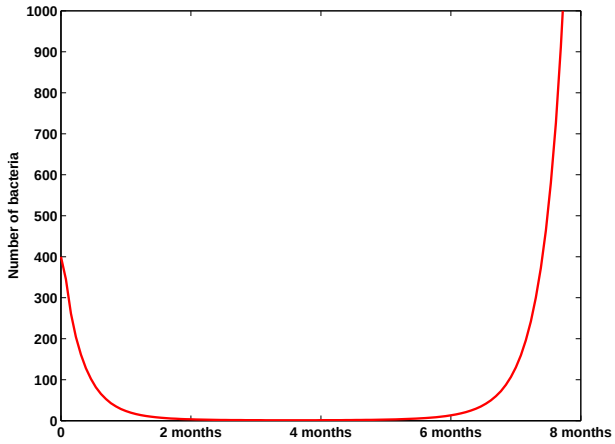

FIGURE 21. Number of bacteria in the first 8 months.

$\lambda_1 = 3 \cdot 10^5$, $\lambda_2 = 7 \cdot 10^5$; d) $\lambda_1 = 3 \cdot 10^5$, $\lambda_2 = 6 \cdot 10^5$. Simulations shows the results in figure 22, where we can observe the number of bacteria increases exponentially in the first three weeks, then it is controlled by the greater immune response.

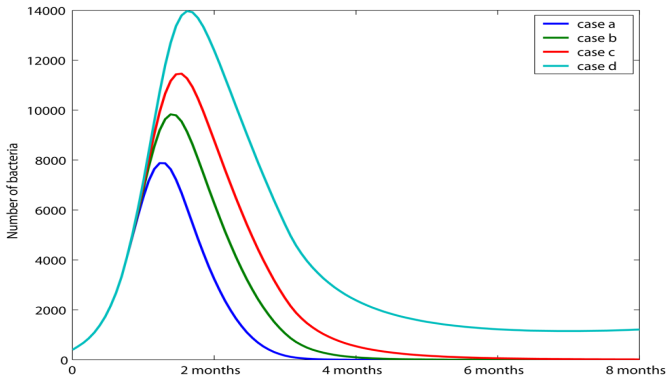

FIGURE 22. Number of bacteria evolution in the first 8 months. Case a: $\lambda_1 = 3 \cdot 10^5$, $\lambda_2 = 1 \cdot 10^6$. Case b): $\lambda_1 = 3 \cdot 10^5$, $\lambda_2 = 8 \cdot 10^5$. Case c):$\lambda_1 = 3 \cdot 10^5$, $\lambda_2 = 7 \cdot 10^5$. Case d):$\lambda_1 = 3 \cdot 10^5$, $\lambda_2 = 6 \cdot 10^5$.

6.2.3. *Granuloma formation.* Finally, we make a long time period simulation, assuming the same conditions of section 6.2.2, except for μ, which is, here, $\mu = 3$ in the first three weeks, and $\mu = 0$ in the following time. This because we suppose that, for a long period of time, the immune system can maintain its efficiency. We can see one-year simulation in figure 23, where the number of bacteria, after an initial growth, is contained, but not canceled by macrophages, its initial value is 400, and its asymptotic value is about 100.

7. **Conclusions.** In this work, we present a qualitative approach to the immune response to Mtb aggression, which is inspired by prey-predator systems. We propose a model, which works in every space dimension, by using mass balances equations

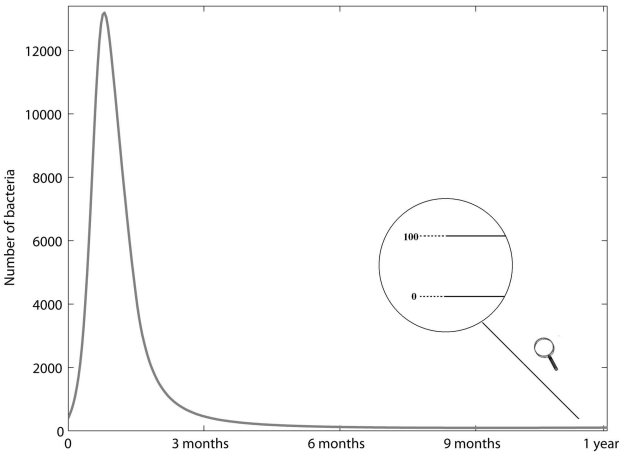

FIGURE 23. Number of bacteria evolution in 1 year.

and a pressure law for the velocity. We find, at least in 1-dimension, a region of linear instability, which is limited by the non-linear terms. We also observe, in long time simulations, the persistence of a small group of bacteria in equilibrium with macrophages. The reactivation mechanism has been also discussed.

Next step will be the development of new models to take into account phagocytosis, activation of cells, T-cells and all the other components which play an important role in the Mtb evolution.

Acknowledgments. The authors wish to thank Denise Kirschner, Simeone Marino and David Gammack for their ideas and suggestions about this topic.

REFERENCES

[1] D. Ambrosi and L. Preziosi, *On the closure of mass balance models for tumor growth*, Math. Models Methods Appl. Sci., **12** (2002), 737–754.

[2] S. Astanin and L. Preziosi, *Multiphase models of tumour growth*, in "Selected Topics on Cancer Modelling: Genesis - Evolution - Immune Competition - Therapy" (eds. N. Bellomo, M. Chaplain and E. De Angelis), Birkhauser (2007), 223–253.

[3] M. Briani, R. Natalini and G. Russo, *Implicit-explicit numerical schemes for jump-diffusion processes*, Calcolo, **44** (2007), 33–57.

[4] G. W. Comstock, *Epidemiology of tuberculosis*, Am. Rev. Respir. Dis., **125** (1982), 8–15.

[5] A. M. Dannenberg and G. A. W. Rook, *Pathogenesis of pulmonary tuberculosis: An interplay of tissue-damaging and macrophage-activating immune responses-dual mechanisms that control bacillary multiplication*, in "Tuberculosis: Pathogenesis, Protection, and Control" (eds. B. R. Bloom), American Society for Microbiology, Washington D.C., (1994), 459–483.

[6] E. De Angelis and L. Preziosi, *Advection-diffusion models for solid tumour evolution in vivo and related free boundary problem*, Math. Models Methods Appl. Sci., **10** (2000), 379–407.

[7] J. L. Flynn and J. Chan, *Tuberculosis: latency and reactivation*, Infect. Immun., **69** (2001), 4195–4201.

[8] D. Gammack, C. R. Doering and D. E. Kirschner, *Macrophage response to mycobacterium tuberculosis infection*, J. Math. Biol., **48** (2004), 218–242.

[9] S. Ganguli, D. Gammack and D. E. Kirschner, *A metapopulation model of granuloma formation in the lung during infection with mycobacterium tuberculosis*, Math. Biosci. Eng., **2** (2005), 535–560.

[10] E. F. Keller and L. A. Segel, *Traveling bands of chemotactic bacteria: A theoretical analysis*, J. Theor. Biol., **30(2)** (1971), 235–248.

[11] D. E. Kirschner and S. Marino, *Mycobacterium tuberculosis as viewed through a computer*, Trends in Microbiology, **13** (2005), 206–211.
[12] F. Krombach, S. Münzing, A. M. Allmeling, J. T. Gerlach, J. Behr and M. Dörger, *Cell size of alveolar macrophages: An interspecies comparison*, Environmental Health Perspectives, **105** Supplement 5: Particle Toxicity (1997), 1261–1263.
[13] D. A. Lauffenburger and J. J. Linderman, "Receptors: Models for Binding, Trafficking, and Signaling," Oxford University Press, New York, 1993.
[14] J. D. Murray, "Mathematical Biology," 3^{rd} edition Springer, (2002).
[15] E. L. Opie and J. D. Aronson, *Tubercle bacilli in latent tuberculous lesions and in lung tissue without tuberculous lesions*, Arch. Path. Lab. Med., **4** (1927), 1–21.
[16] M. R. Owen and J. A. Sherratt, *Pattern formation and spatiotemporal irregularity in a model for macrophage-tumour interactions*, J. Theor. Biol., **189** (1997), 63–80.
[17] M. R. Owen and J. A. Sherratt, *Mathematical modelling of macrophage dynamics in tumours*, Math. Models Meth. Appl. Sci., **9** (1999), 513–539.
[18] L. Preziosi and S. Astanin, *Modelling the formation of capillaries*, in "Integration of Complex Systems in Biomedicine" (eds. A. Quarteroni), Springer, (2005), 109–145.
[19] H. E. Robertson, *Persistence of tuberculous infection*, Am. J. Pathol., **9** (1933), S711–S718.
[20] S. J. Ruuth, *Implicit explicit methods for reaction-diffusion problems in pattern formation*, J. Math, Bio., **34** (1995), 148–176.
[21] P. Sannomiya, R. A. Craig, D. B. Clewell, A. Suzuki, M. Fujino, G. O. Till and W. A. Marasco, *Characterization of a class of nonformylated enterococcus faecalis-derived neutrophil chemotactic peptides: the sex pheromones*, Proc. Natl. Acad. Sci. USA, **87** (1990), 66–70.
[22] S. Sozzani, W. Luini, M. Molino, P. Jìlek, B. Bottazzi, C. Cerletti, K. Matsushima and A. Mantovani, *The signal transduction pathway involved in the migration induced by a monocyte chemotactic cytokine*, J. Immunol., **147** (1991), 2215–2221.
[23] F. D. Stickle, D. A. Lauffenburger and R. P. Daniele, *The motile response of lung macrophages: Theoretical and experimental approaches using the linear under-agarose assay*, J. Leukocite Biology, **38** (1985), 383–401.
[24] J. E. Wigginton and E. D. Kirschner, *A model to predict cell-mediated immune regulatory mechanisms during human infection with mycobacterium tuberculosis*, J. Immunol., **166** (2001), 1951–1967.
[25] World Health Organization (WHO), "Tuberculosis Fact Sheet N-104: Global and Regional Incidence," March 2006, Retrieved on 6 October 2006.
[26] M. Zhang, J. Gong, Y. Lin and P. F. Barnes, *Growth of virulent and avirulent mycobacterium tuberculosis strains in human macrophages*, Infect. Immun., **66** (1998), 794–799.

Received January 5, 2009; Accepted October 26, 2009.

E-mail address: f.clarelli@iac.rm.cnr.it
E-mail address: r.natalini@iac.rm.cnr.it